

**Conformational Changes Spanning Angstroms to Nanometers
via a Combined Protein Induced Fluorescence Enhancement-
Förster Resonance Energy Transfer Method**

Yasser Gidi,[‡] Matthias Götze[†] and Gonzalo Cosa^{,‡}*

[‡] Department of Chemistry and Center for Self-Assembled Chemical Structures (CSACS-CRMAA), McGill University, 801 Sherbrooke Street West, Montreal, QC H3A 0B8, Canada.

[†] Department of Biochemistry, Department of Medical Microbiology and Immunology, University of Alberta, 6020K Katz Group Centre, Edmonton, AB T6G 2E1, Canada

*** To whom correspondence should be addressed:**

Email: gonzalo.cosa@mcgill.ca

This supplementary information section includes:

- i. Modifications to Oligonucleotides and Spectral Discrimination of Dyes**
- ii. Revision of the Most Important Equations Used in FRET**
- iii. Extracting Changes in the Fluorescence Quantum Yield from FRET Traces**
- iv. Determination of γ from SMF Experiments Considering Donor-acceptor Cross-talk and Direct Excitation of the Acceptor**

- v. **Apparent FRET Efficiency Correction due to Crosstalk and Direct Excitation of the Acceptor**
- vi. **Distribution of E_{pr} Values Recorded from smFRET TIRF Experiments after Correction for Crosstalk and before Correction for Direct Excitation of the Acceptor.**
- vii. **Correction Parameters Utilized to Correct Single-Molecule Data**
- viii. **smPIFE TIRF Trajectories of Cy3/R₂₀^A in the Presence of 100 nM NS5B**
- ix. **References**

i. Modifications to Oligonucleotides and Spectral Discrimination of Dyes

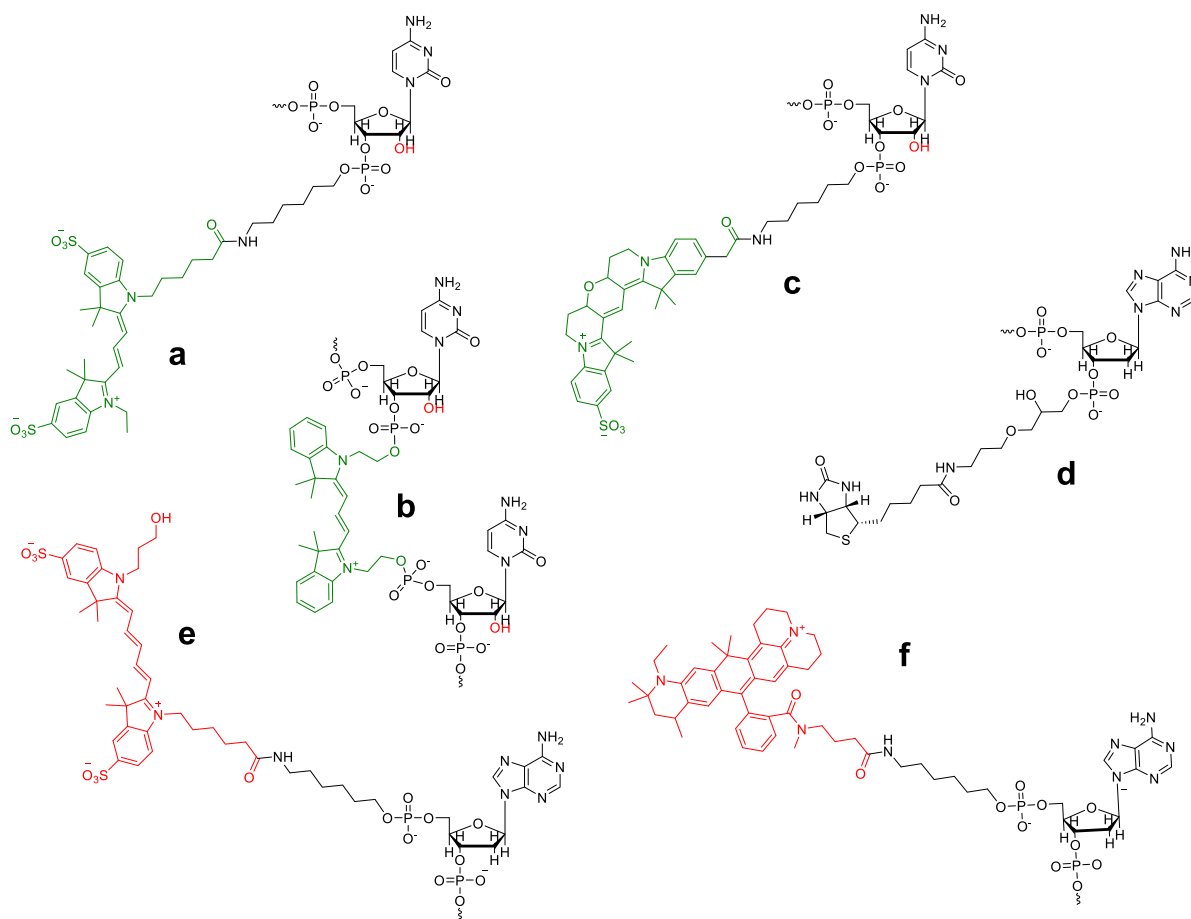


Figure S1. Dyes and Modifications Utilized: Chemical structure of the various dye conjugates utilized, Cy3 and Cy3B appear in green and Cy5 and ATTO647N in red. Conjugate (a) utilized in R_{20}^S is a cytidylate terminated 3' overhang with Cy3 tethered to the phosphate at position 3' of the ribose via a succinimide linker. Conjugate (b) utilized in R_{20}^A is an internal Cy3 tethered to the phosphate backbone (internal amidite). Conjugate (c) utilized in R_{20}^S is a cytidylate terminated 3' overhang with Cy3B tethered to the phosphate at position 3' of the ribose via a succinimide linker. Structure (d) shows the biotin conjugation at the 3' end of the DNA strand. (e)

and (f) correspond to Cy5 and ATTO647N¹ conjugates at the 5' end of the DNA strand respectively.

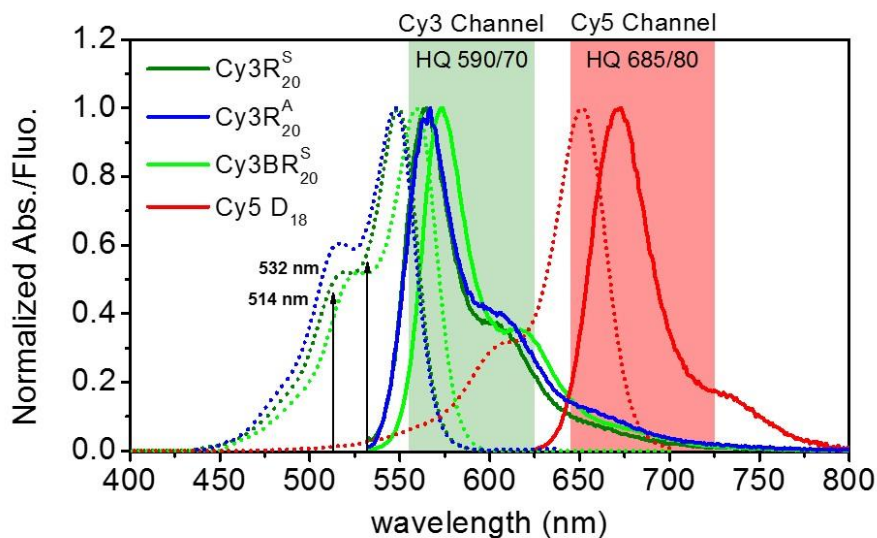


Figure S2. Cy3, Cy3B and Cy5 Spectral Discrimination. Absorbance (dotted line) and fluorescence (solid line) spectra of Cy3 (green) Cy3B (light green) and Cy5 (red) labeled oligonucleotides. Superimposed on the spectra are the bandpass profiles for the emission filters utilized for the Cy3 and Cy5 channels.

ii. Revision of the Most Important Equations Used in FRET

The rate constant of energy transfer k_T was defined by Förster as shown in **equation (1)** below.^{2, 3-4} It depends on the spectral overlap integral between *donor* and *acceptor* dyes $J(\lambda)$, the fluorescence quantum yield of the donor in the absence of acceptor Φ_f^D , the donor lifetime in the absence of acceptor τ_d^D , the refractive index of the medium n , the Avogadro's number N_A , the geometric factor κ^2 which accounts for the relative dipole orientation between the donor and acceptor and the interfluorophore distance r . The Förster Radius R_0 , defined as the distance r at

which 50 percent of the energy is transferred to the acceptor, is described by **equation (2)**. Combining **equations (1) and (2)**, the rate of energy transfer may be written as shown in **equation (3)**.

$$k_T = \frac{\phi_f^D \kappa^2}{\tau_d^D r^6} \left(\frac{9000(\ln 10)}{128\pi^5 N_A n^4} \right) J(\lambda) \quad (1)$$

$$R_0 = \left(\phi_f^D \kappa^2 \left(\frac{9000(\ln 10)}{128\pi^5 N_A n^4} \right) J(\lambda) \right)^{1/6} \quad (2)$$

$$k_T = \frac{1}{\tau_d^D} \left(\frac{R_0}{r} \right)^6 \quad (3)$$

The energy transfer efficiency E , defined as the fraction of the donor excitation that is transferred to the acceptor, is given by **equation (4)**.⁵ Where k_r is the radiative decay rate constant and k_{nr} is the sum of all other non-radiative decay rates constants (excluding energy transfer). Several methods have been utilised to measure FRET Efficiency. It may be calculated from the donor emission intensity as shown in **equation (5)**, where ϕ_f^D and ϕ_f^{DA} are the fluorescence quantum yields of the donor in the absence and presence of acceptor, respectively. Intensities (I^D and I^{DA}) or lifetimes (τ_d^D and τ_d^{DA}) can be used instead of quantum yield.

$$E = \frac{k_T}{k_T + k_r + k_{nr}} = \frac{1}{1 + \left(\frac{r}{R_0} \right)^6} \quad (4)$$

$$E = 1 - \frac{\phi_f^{DA}}{\phi_f^D} = 1 - \frac{I^{DA}}{I^D} = 1 - \frac{\tau_d^{DA}}{\tau_d^D} \quad (5)$$

Provided that the acceptor is fluorescent, E may also be obtained using **equation (6)** below, where I_D and I_A^{exp} are the background corrected experimental intensities of the donor and acceptor respectively.⁶

In order to obtain accurate values for E , corrections must be applied to account for crosstalk (leakage) of the donor into the acceptor channel, differences in the donor and acceptor quantum yields of fluorescence and differences in the detection efficiencies of the two channels (**Supplementary Figure 3**).⁷⁻⁸ In some cases, direct excitation of the acceptor I_A^{DE} can also be taken into account, especially when efficiency is low and direct excitation becomes an important part of the acceptor signal. In **equation (6)** βI_D corrects for the crosstalk of donor emission into the acceptor channel and I_A^{DE} for direct excitation of the acceptor. I_A is then the fully corrected acceptor intensity. The parameter γ as shown in **equation (7)** accounts for the differences in the fluorescence quantum yield Φ_f and detection efficiency η of donor and acceptor channels.

$$E = \frac{I_A^{exp} - \beta I_D - I_A^{DE}}{I_A^{exp} - \beta I_D - I_A^{DE} + \gamma I_D} = \frac{I_A}{I_A + \gamma I_D} \quad (6)$$

$$\gamma = \frac{\eta_A}{\eta_D} \frac{\Phi_f^A}{\Phi_f^D} \quad (7)$$

Correction parameters β and γ can be calculated from single molecule intensity-time trajectories.^{5, 9-11} The correction factor γ is equivalent to $-\Delta I_A^{exp} / \Delta I_D^{exp}$ when there is neither crosstalk from the donor to the acceptor channel nor direct excitation of the acceptor (**see Figure S3** and text therein), where ΔI_A^{exp} and ΔI_D^{exp} are the acceptor and donor intensity changes, respectively when acceptor photobleaching occurs. β is determined according to I_A' / I_D' , where I_A'

and I'_D are the intensities in the acceptor and donor channels respectively, corrected for background and recorded following acceptor photobleaching and prior to donor photobleaching.

The most frequently used single-molecule spectroscopy analysis based on FRET to monitor distance-conformational fluctuations uses the ratiometric method as an approximation to the real FRET efficiency. This analysis represents the ratio between the acceptor detected fluorescence and the total detected fluorescence (donor + acceptor). When intensities are neither corrected for background nor for crosstalk the result has been termed proximity factor P ¹², proximity ratio P ¹³ PR¹⁴ or relative proximity ratio E_{pr} ⁹. When intensities are corrected for background and crosstalk it has been called apparent FRET efficiency E_{app} .¹⁵⁻¹⁶ Recently, proximity ratio E_{pr} has been amply adopted with a new computation involved, where intensities are corrected for both background and crosstalk.¹⁷⁻¹⁹ In this work we have adopted E_{pr} in its new definition as the nomenclature of use. In this specific case, we have also corrected by direct excitation (see **equation (8)**).

$$E_{pr} = \frac{I_A^{exp} - \beta I_D - I_A^{DE}}{I_A^{exp} - \beta I_D - I_A^{DE} + I_D} = \frac{I_A}{I_A + I_D} \quad (8)$$

In utilizing the above equation to calculate FRET efficiency E , it is assumed that $\eta_D \Phi_f^D = \eta_A \Phi_f^A$. This method provides an apparent value for E as recognized in the published literature.

iii. Extracting Changes in the Fluorescence Quantum Yield from FRET Traces

In single molecule experiments, depending on the power of the excitation source, a fluorescent dye may usually undergo several excitation cycles per second and therefore it is convenient to focus in the quanta of energy absorbed, transferred, lost as heat or emitted per second. In the case of absorption and emission processes, those quantum of energy are called photons. For convenience we will discuss the rates (ν) of the processes to differentiate them from the rate constants (k) (k_r for radiative and k_{nr} for non-radiative processes). These new rates (ν) may change over the course of the experiment as they will depend on the flux of photons from the excitation source (laser excitation power for the donor and energy transfer rate for the acceptor).

The excitation rate ν_{ex} is the number of times a molecule is excited per unit time. The radiative rates ν_r^D and ν_r^A are the number of times the excited donor and acceptor respectively, emit a photon per unit time. Non-radiative rates ν_{nr}^D and ν_{nr}^A are the number of times the excited donor and acceptor respectively deactivate the excited state through non-radiative processes, excluding energy transfer. Finally, ν_T is the number of times the donor can transfer a quantum of energy to the acceptor per unit time (see **Figure 1**)

A kinetic balance may be obtained from all the processes that populate and depopulate the excited state. The rate of excitation of the donor is equal to the sum of the rates for all the processes that depopulate the excited state of the donor. In the absence of an acceptor, the excited state is depopulated by radiative (emission of a photon) and non-radiative processes (all other paths) as

shown by **equation (9)**, where $I_{ex}(t)$ and σ_D are the excitation flux of photons ($s^{-1} cm^{-2}$) and the absorption cross section on the donor (cm^2) respectively.

$$I_{ex}(t)\sigma_D = v_{ex}^D = v_{nr}^D + v_r^D \quad (9)$$

The fluorescence quantum yield of the donor can be written as:

$$\Phi_f^D = \frac{k_r^D}{k_{nr}^D + k_r^D} = \frac{v_r^D}{v_{nr}^D + v_r^D} \quad (10)$$

In the presence of an acceptor, a new deactivation process involving energy transfer to the acceptor dye is added to the excited donor, therefore the new balance is:

$$v_{ex}^D = v_{nr}^D + v_r^D + v_T \quad (11)$$

As shown in **equation (9)** (main manuscript), only a fraction of the energy transferred from the donor to the acceptor will be converted into photons, this fraction is given by the quantum yield of fluorescence of the acceptor dye.

$$\Phi_f^A = v_r^A / v_T \quad (12)$$

Replacing **equations (12)** and **(10)** in **(11)** will yield **equation (13)**. This equation is valid independently of the rate v_T of energy transfer.

$$v_{ex}^D = \frac{v_r^D}{\Phi_f^D} + \frac{v_r^A}{\Phi_f^A} \quad (13)$$

In order to convert v_r^D to rates of photon detection for the acceptor ($I_A(t)$) and donor ($I_D(t)$), it is necessary to correct for a detection efficiency factor accounting for the collection efficiency of the objective, losses due to reflection at multiple interfaces and quantum detection efficiency of the detector utilized. Then $v_r^D = I_D(t)/\eta_D$ and $v_r^A = I_A(t)/\eta_A$. Replacing in **equation (13)**, we obtain **equation (14)**. Multiplying **equation (14)** by $\eta_A\Phi_f^A$ and using the definition of γ in **equation (7)** will lead to **equation (15)**.

$$v_{ex}^D = \frac{I_D(t)}{\eta_D\Phi_f^D} + \frac{I_A(t)}{\eta_A\Phi_f^A} \quad (14)$$

$$v_{ex}^D\eta_A\Phi_f^A = \frac{\eta_A\Phi_f^A}{\eta_D\Phi_f^D}I_D(t) + I_A(t) = \gamma I_D(t) + I_A(t) \quad (15)$$

Armed with **equation (15)**, the fluorescence quantum yield of the donor can be written in terms of the initial fluorescence quantum yield of the donor and a factor D accounting for fluctuations in Φ_f^D over time (**equation (16)**). Replacing **equation (16)** in **(15)** yield **equation (17)**.

$$\Phi_f^D = D\Phi_f^{D_0} \quad (16)$$

$$v_{ex}^D\eta_A\Phi_f^A = \frac{\eta_A\Phi_f^A}{\eta_DD\Phi_f^{D_0}}I_D(t) + I_A(t) = \frac{\gamma_0}{D}I_D(t) + I_A(t) \quad (17)$$

Note that γ_0 is defined as a fixed initial parameter and it does not depend on variations of the fluorescence quantum yield of the donor. If the rate of the donor excitation v_{ex}^D , detection

efficiency η_A and fluorescence quantum yield of the acceptor Φ_f^A remain constant, the left side of **equation (17)** is a constant, and then the right side of the **equation (17)** should also remain constant. Using an initial value of $D = D_0 = 1$, an initial condition can be calculated as:

$$\left(v_{ex}^D \eta_A \Phi_f^A\right)_0 = X_0 = \gamma_0 I_{D_0} + I_{A_0} \quad (18)$$

As discussed above X_0 will remain constant over the course of the experiment, provided that $\Delta \left(v_{ex}^D \eta_A \Phi_f^A\right) = 0$. **Equation (17) and (18)** can then be combined to yield:

$$\gamma_0 I_{D_0} + I_{A_0} = X_0 = \frac{\gamma_0}{D} I_D(t) + I_A(t) \quad (19)$$

Rearranging **equation (19)**, the factor D by which the fluorescence quantum yield of the donor is varied, can be calculated as:

$$D = \frac{I_D(t)\gamma_0}{\gamma_0 I_{D_0} + I_{A_0} - I_A(t)} = \frac{I_D(t)\gamma_0}{X_0 - I_A(t)} \quad (20)$$

Similarly, an equation to track changes in the fluorescence quantum yield of the acceptor, assuming that Φ_f^D is constant, can be derived from **equation (14)** where $\Phi_f^A = A\Phi_f^{A_0}$.

$$v_{ex}^D \eta_D \Phi_f^D = I_D(t) + \frac{\eta_D \Phi_f^D}{\eta_A A \Phi_f^{A_0}} I_A(t) \quad (21)$$

Using **equation (8)**, **equation (21)** can be reduced to:

$$v_{ex}^D \eta_D \Phi_f^D = I_D(t) + \frac{1}{A\gamma_0} I_A(t) \quad (22)$$

Using an initial value of $A = 1$, the initial condition can be calculated as:

$$(v_{ex}^D \eta_D \Phi_f^D)_0 = Y_0 = I_{D_0} + \frac{1}{\gamma_0} I_{A_0} \quad (23)$$

Rearranging the **equation (23)**, the factor A by which the fluorescence quantum yield of the acceptor is varied, can be calculated as:

$$A = \frac{I_A(t)}{\gamma_0(Y_0 - I_D(t))} \quad (24)$$

iv. **Determination of γ from SMF Experiments Considering Donor-acceptor Cross-talk and Direct Excitation of the Acceptor**

The parameter γ is typically determined following photobleaching of the acceptor, where the experimentally observed anticorrelated changes in the donor and acceptor signals, ΔI_D^{exp} and ΔI_A^{exp} , respectively, are measured and used in the calculation, according to **equation (25)** see also **Fig. S3**. This equation assumes that the recorded changes are purely due to deactivation of FRET energy transfer following photodestruction of the acceptor chromophore, where quanta not

delivered to and emitted in the acceptor channel are in turn available for emission from the donor channel.

$$\gamma = -\frac{\Delta I_A^{exp}}{\Delta I_D^{exp}} \quad (25)$$

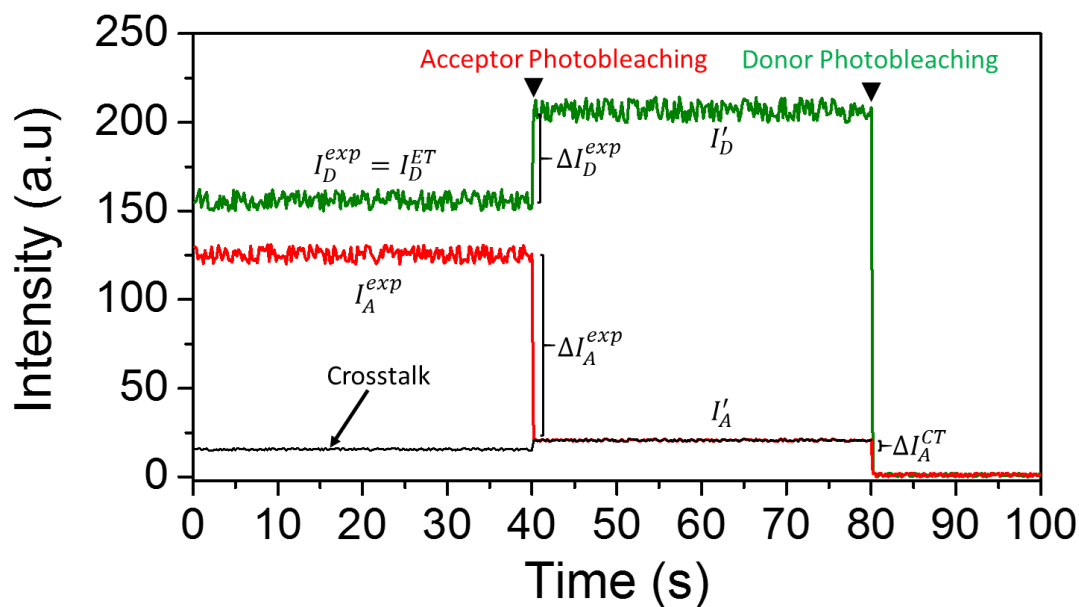


Figure S3. Measurement of γ from the Donor and Acceptor Intensity-time Trajectories.

Representation of traces for a donor-acceptor pair where γ can be calculated upon the anti-correlated change in acceptor (red) and donor (green) intensity when the acceptor photobleaches. Acceptor and donor photobleaching are indicated with inverted triangles ▼. The black trace represents an imaginary trace for the leakage and its respective change after a donor change in intensity. ($\beta = 0.1$, $\gamma = 2.16$)

The experimental change in the donor channel, ΔI_D^{exp} , is purely the result of the deactivation of emissive losses from the donor that takes place via energy transfer from the donor

to the acceptor channel ΔI_D^{ET} . This deactivation upon acceptor photobleaching results in an increase in intensity (**equation (26)**). In turn, the intensity drop in the acceptor channel, ΔI_A^{exp} , may contain elements from donor acceptor cross-talk as well as from the direct excitation of the acceptor, not considered in **equation (25)**. The experimentally observed change in the acceptor signal will then be given by **equation (27)**, where ΔI_D^{ET} accounts for energy transfer from the donor dye to the acceptor dye via dipole-dipole interaction and where a parameter ΔI_A^{CT} is introduced accounting for donor cross-talk into the acceptor channel. A second parameter ΔI_A^{DE} is introduced to account for direct excitation of the acceptor by the laser line. The parameter γ is then given by **equation (28)**.

$$\Delta I_D^{exp} = \Delta I_D^{ET} \quad (26)$$

$$\Delta I_A^{exp} = \Delta I_A^{ET} - \Delta I_A^{CT} + \Delta I_A^{DE} \quad (27)$$

$$\gamma = \frac{\Delta I_A^{ET}}{\Delta I_D^{ET}} = \frac{\Delta I_A^{ET}}{\Delta I_D^{exp}} \quad (28)$$

Utilizing **equations (26)** and **(27)**, the experimental change in the acceptor channel over the donor channel can be written as shown below in **equation (29)**. It may be appreciated that the first term to the right in **equation (29)** corresponds to γ . In turn, the second and third term may be computed. Specifically, one may show that the change in cross talk signal in the acceptor channel ΔI_A^{CT} upon acceptor photobleaching is directly proportional to the simultaneous increase in donor signal ΔI_D^{exp} upon acceptor photobleaching, where the proportionality constant is β , see **equation (30)** and also **equation (6)** and text therein. Then, the second term to the right is equal to β .

The third term to the right may be calculated from a simple consideration based on the absorption cross section values for the donor σ_D and acceptor σ_A dye dyes at the donor excitation wavelength, see **equation (31)**. Specifically, the emission arising upon direct excitation of the acceptor (constant throughout the experiment in as far as Φ_f^A remains constant) I_A^{DE} should be proportional to that arising upon direct excitation of the donor. The latter is given by I_D' , see **Figure S3**. The proportionality constant is given by the correction factor due to fluorescence quantum yield and detection efficiencies for both dyes γ , and the correction factor for differences in cross section for both dyes, $\sigma_A/\sigma_D = \varepsilon_A/\varepsilon_D$, where ε_D and ε_A are the absorption coefficients at the excitation wavelength of the experiment. In turn, one may show that following acceptor photobleaching, the change in intensity from direct excitation is equal to the intensity arising from direct excitation $\Delta I_A^{DE} = I_A^{DE}$.

$$\frac{\Delta I_A^{exp}}{\Delta I_D^{exp}} = \frac{\Delta I_A^{ET}}{\Delta I_D^{exp}} - \frac{\Delta I_A^{CT}}{\Delta I_D^{exp}} + \frac{\Delta I_A^{DE}}{\Delta I_D^{exp}} \quad (29)$$

$$\Delta I_A^{CT} = \beta \Delta I_D^{exp} \quad (30)$$

$$\Delta I_A^{DE} = I_A^{DE} = I_D' \gamma \frac{\sigma_A}{\sigma_D} = I_D' \gamma \frac{\varepsilon_A}{\varepsilon_D} \quad (31)$$

Replacing **equations (28), (30) and (31)** in **equation (29)** gives:

$$\frac{\Delta I_A^{exp}}{\Delta I_D^{exp}} = \gamma - \beta + \gamma \frac{I_D'}{\Delta I_D^{exp}} \frac{\varepsilon_A}{\varepsilon_D} \quad (32)$$

Rearranging for γ , we obtain the desired equation to determine γ following acceptor photobleaching.

$$\gamma = \frac{\frac{\Delta I_A^{exp}}{\Delta I_D^{exp}} + \beta}{1 + \frac{I_D'}{\Delta I_D^{exp}} \frac{\epsilon_A}{\epsilon_D}} \quad (33)$$

v. Apparent FRET Efficiency Correction due to Crosstalk and Direct Excitation of the Acceptor

In order to obtain proximity ratio E_{pr} as defined in **section ii**, the background subtracted intensity of the acceptor I_A^{exp} must be corrected for both donor-acceptor crosstalk and direct excitation of the acceptor. Corrections require subtracting the contribution from both those phenomena (I_A^{CT} and I_A^{DE}) to the experimental intensity recorded for the acceptor channel I_A^{exp} . The acceptor intensity due to energy transfer I_A^{ET} will then be given by **equation (34)**. The contribution from cross-talk can be expressed as βI_D^{exp} (see also **equation (30)**). The contribution due to direct excitation of the acceptor can be calculated according to **equation (31)**. Replacing those values in **equation (34)** yields **equation (35)**.

$$I_A^{ET} = I_A^{exp} - I_A^{CT} - I_A^{DE} \quad (34)$$

$$I_A^{ET} = I_A^{exp} - \beta I_D^{exp} - I_D' \gamma \frac{\epsilon_A}{\epsilon_D} \quad (35)$$

The parameter β may be calculated experimentally from single molecule trajectories after photobleaching of the acceptor and prior to photobleaching of the donor as described in the

literature.^{5, 9-11} I_A^{DE} can be calculated from each trajectory using a combination of **equation (32)** and **(33)**, as shown in **equation (36)**

$$I_A^{DE} = I_D' \gamma \frac{\varepsilon_A}{\varepsilon_D} = I_D' \frac{\varepsilon_A}{\varepsilon_D} \left(\frac{-\frac{\Delta I_A^{exp}}{\Delta I_D^{exp}} + \beta}{1 + \frac{I_D' \varepsilon_A}{\Delta I_D^{exp} \varepsilon_D}} \right) \quad (36)$$

It is now possible to define E_{pr} as shown in **equation (37)**, where I_D^{exp} and I_A^{exp} are the experimental donor and acceptor intensities, respectively.

$$E_{pr} = \frac{I_A^{ET}}{I_D^{ET} + I_A^{ET}} = \frac{I_A^{exp} - I_A^{CT} - I_A^{DE}}{I_D^{exp} + I_A^{exp} - I_A^{CT} - I_A^{DE}} \quad (37)$$

Alternatively, and for cases where donor photobleaches first, I_A^{DE} can be calculated according to **equations (38-41)** using the known γ . Here **equation (38)** may be directly inferred from **equation (19)**.

$$I_D^{exp} + \frac{I_A^{ET}}{\gamma} = I_D' \quad (38)$$

Combining **equations (31) and (38)** gives:

$$I_A^{DE} = (\gamma I_D^{exp} + I_A^{ET}) \frac{\varepsilon_A}{\varepsilon_D} \quad (39)$$

Combining **equations (35) and (39)** gives:

$$I_A^{DE} = \left(\gamma I_D^{exp} + I_A^{exp} - \beta I_D^{exp} - I_A^{DE} \right) \frac{\varepsilon_A}{\varepsilon_D} \quad (40)$$

Reorganizing **equation (40)** for I_A^{DE} and using $f = (1 + \varepsilon_D/\varepsilon_A)^{-1}$ results in a new expression for I_A^{DE} , **equation (41)**.

$$I_A^{DE} = f((\gamma - \beta)I_D^{exp} + I_A^{exp}) \quad (41)$$

vi. **Distribution of E_{pr} Values Recorded from smFRET TIRF Experiments after Correction for Crosstalk and before Correction for Direct Excitation of the Acceptor.**

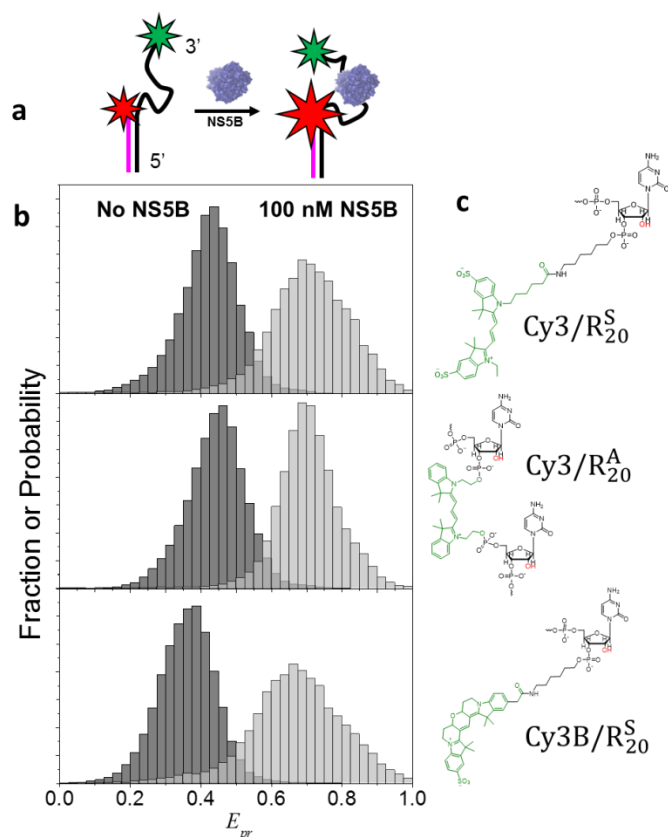


Figure S4. Distribution of E_{pr} Values Recorded from smFRET TIRF Experiments Before Direct Acceptor Excitation Corrections. **a.** Cartoon illustrating a DNA/RNA duplex before (left) and after (right) HCV-NS5B binding. **b.** Uncorrected ensemble histograms of single-molecule E_{pr} values for DNA/RNA duplexes before (left) and after (right) HCV-NS5B binding. **c.** chemical structures of the linkers utilized to couple the donor (either Cy3 or Cy3B) in Cy3B/R₂₀^S, Cy3/R₂₀^A and Cy3/R₂₀^S.

vii. Correction Parameters Utilized to Correct Single-Molecule Data

Table S1: Correction Parameters

dye pair/ R_n^X	Crosstalk (β)	Gamma (γ)	ϵ_D/ϵ_A (532nm)
Cy3 – Cy5/ R_{20}^S ^a	0.09 ± 0.04 (74)	2.6 ± 0.6 (52)	86823/6723
Cy3 – Cy5/ R_{20}^A ^b	0.08 ± 0.02 (225)	1.3 ± 0.3 (127)	97893/6723
Cy3B–Cy5/ R_{20}^S ^c	0.08 ± 0.02 (105)	0.37 ± 0.04 (57)	77586/6723
Cy3–ATTO647N/ R_{26}^A ^b	-	2.6 ± 0.4 (94)	97893/4500

Superscripts letters indicate the structure of the dye in **Figure S1**. Parenthesis indicate the number of trajectories utilized.

viii. smPIFE TIRF Trajectories of Cy3/ R_{20}^A in the Presence of 100 nM NS5B

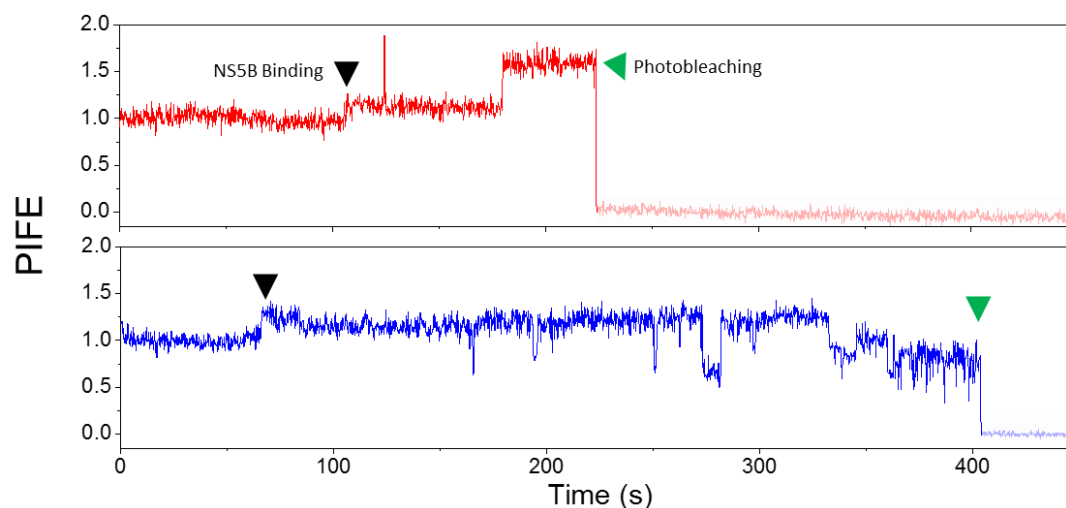


Figure S5. smPIFE Trajectories of Cy3/ R_{20}^A when Flowing 100 nM NS5B. Normalized trajectories representing different Cy3 photophysical behaviours (associated to different binding modes) upon NS5B binding to Cy3/ R_{20}^A . The red trace displays an enhancement-only trajectory. The blue trace shows a trajectory where enhancement and quenching of Cy3 are both recorded in the presence of NS5B.

ix. REFERENCES:

- (1) Eggeling, C.; Ringemann, C.; Medda, R.; Schwarzmann, G.; Sandhoff, K.; Polyakova, S.; Belov, V. N.; Hein, B.; von Middendorff, C.; Schonle, A.; Hell, S. W. Direct observation of the nanoscale dynamics of membrane lipids in a living cell. *Nature* **2009**, *457*, 1159-1162.
- (2) Förster, T. Zwischenmolekulare Energiewanderung und Fluoreszenz (Intermolecular Energy Migration and Fluorescence). *Annalen der Physik* **1948**, *437*, 55-75. Translated by RS Knox, Department of Physics and Astronomy, University of Rochester, Rochester, NY 14627.
- (3) Lakowicz, J. R., *Principles of Fluorescence Spectroscopy*. 3 ed.; Springer: 2006; Vol. 2, p 954.
- (4) Braslavsky, S. E.; Fron, E.; Rodriguez, H. B.; Roman, E. S.; Scholes, G. D.; Schweitzer, G.; Valeur, B.; Wirz, J. Pitfalls and Limitations in the Practical Use of Forster's Theory of Resonance Energy Transfer. *Photochem. Photobiol. Sci.* **2008**, *7*, 1444-1448.
- (5) Ha, T.; Ting, A. Y.; Liang, J.; Chemla, D. S.; Schultz, P. G.; Weiss, S.; Deniz, A. A. Temporal fluctuations of fluorescence resonance energy transfer between two dyes conjugated to a single protein. *Chem. Phys.* **1999**, *247*, 107-118.
- (6) Sabanayagam, C. R.; Eid, J. S.; Meller, A. Using fluorescence resonance energy transfer to measure distances along individual DNA molecules: Corrections due to nonideal transfer. *J. Chem. Phys.* **2005**, *122*, 061103.
- (7) Dahan, M.; Deniz, A. A.; Ha, T.; Chemla, D. S.; Schultz, P. G.; Weiss, S. Ratiometric Measurement and Identification of Single Diffusing Molecules. *Chem. Phys.* **1999**, *247*, 85-106.
- (8) Deniz, A. A.; Dahan, M.; Grunwell, J. R.; Ha, T.; Faulhaber, A. E.; Chemla, D. S.; Weiss, S.; Schultz, P. G. Single-Pair Fluorescence Resonance Energy Transfer on Freely Diffusing

Molecules: Observation of Förster Distance Dependence and Subpopulations. *Proc. Natl. Acad. Sci. U. S. A.* **1999**, *96*, 3670-3675.

(9) McCann, J. J.; Choi, U. B.; Zheng, L.; Weninger, K.; Bowen, M. E. Optimizing Methods to Recover Absolute FRET Efficiency from Immobilized Single Molecules. *Biophys. J.* *99*, 961-970.

(10) Ha, T.; Ting, A. Y.; Liang, J.; Caldwell, W. B.; Deniz, A. A.; Chemla, D. S.; Schultz, P. G.; Weiss, S. Single-molecule fluorescence spectroscopy of enzyme conformational dynamics and cleavage mechanism. *Proc. Natl. Acad. Sci. U. S. A.* **1999**, *96*, 893-898.

(11) Sabanayagam, C. R.; Eid, J. S.; Meller, A. High-throughput scanning confocal microscope for single molecule analysis. *Appl. Phys. Lett.* **2004**, *84*, 1216-1218.

(12) Ha, T.; Zhuang, X.; Kim, H. D.; Orr, J. W.; Williamson, J. R.; Chu, S. Ligand-induced conformational changes observed in single RNA molecules. *Proc. Natl. Acad. Sci. U. S. A.* **1999**, *96*, 9077-9082.

(13) Ying, L.; Wallace, M. I.; Balasubramanian, S.; Klenerman, D. Ratiometric Analysis of Single-Molecule Fluorescence Resonance Energy Transfer Using Logical Combinations of Threshold Criteria: A Study of 12-mer DNA. *J. Phys. Chem. B* **2000**, *104*, 5171-5178.

(14) Nir, E.; Michalet, X.; Hamadani, K. M.; Laurence, T. A.; Neuhauser, D.; Kovchegov, Y.; Weiss, S. Shot-Noise Limited Single-Molecule FRET Histograms: Comparison between Theory and Experiments†. *J. Phys. Chem. B* **2006**, *110*, 22103-22124.

(15) Roy, R.; Hohng, S.; Ha, T. A Practical Guide to Single-Molecule FRET. *Nat. Meth* **2008**, *5*, 507-516.

(16) Shirude, P. S.; Balasubramanian, S. Single molecule conformational analysis of DNA G-quadruplexes. *Biochimie* **2008**, *90*, 1197-1206.

- (17) Hohlbein, J.; Craggs, T. D.; Cordes, T. Alternating-laser excitation: single-molecule FRET and beyond. *Chem. Soc. Rev.* **2014**, *43*, 1156-1171.
- (18) Lee, N. K.; Kapanidis, A. N.; Wang, Y.; Michalet, X.; Mukhopadhyay, J.; Ebright, R. H.; Weiss, S. Accurate FRET Measurements within Single Diffusing Biomolecules Using Alternating-Laser Excitation. *Biophys. J.* **2005**, *88*, 2939-2953.
- (19) Ploetz, E.; Lerner, E.; Husada, F.; Roelfs, M.; Chung, S.; Hohlbein, J.; Weiss, S.; Cordes, T. Förster Resonance Energy Transfer and Protein-Induced Fluorescence Enhancement as Synergetic Multi-Scale Molecular Rulers. *Sci. Rep.* **2016**, *6*, 33257.